Overexpression of salusin-α upregulates AdipoR2 and activates the PPARα/ApoA5/SREBP-1c pathway to inhibit lipid synthesis in HepG2 cells

HUAN ZHANG[1*], CHAO YANG[1*], SONGJIAO WANG[2], AOHONG XU[1], QIAN ZHANG[3], XIUQUN DUAN[2], GUOFU GONG[2*] and YUXUE WANG[1*]

[1]Department of Laboratory Medicine, Hubei University of Chinese Medicine, Wuhan, Hubei 430065; [2]Department of Clinical Laboratory, Ezhou Central Hospital, Ezhou, Hubei 436000; [3]Department of Emergency, Xiangyang Central Hospital, Xiangyang, Hubei 441032, P.R. China

Received November 30, 2022; Accepted March 27, 2023

DOI: 10.3892/ijmm.2023.5244

Abstract. Salusin-α and adiponectin, are vasoactive peptides with numerous similar biological effects related to lipid metabolism. Adiponectin has been shown to reduce fatty acid oxidation and to inhibit lipid synthesis of liver cells through its receptor, adiponectin receptor 2 (AdipoR2), but whether salusin-α is able to interact with AdipoR2, was not previously reported. To investigate this, *in vitro* experiments were carried out. The overexpression and interference recombinant plasmids were constructed with salusin-α. The lentiviral expression systems of salusin-α overexpression and interference were respectively synthesized in 293T cells, and 293T cells were infected with the lentivirus. Finally, the association between salusin-α and AdipoR2 was analyzed by semi-quantitative PCR. Subsequently, HepG2 cells were also infected with these viruses. The expression levels of AdipoR2, peroxisome proliferator-activated receptor-α (PPARα), apolipoprotein A5 (ApoA5) and sterol regulatory element-binding transcription factor 1 (SREBP-1c) were detected by western blotting, and AdipoR2 inhibitor (thapsigargin) and agonist [4-phenyl butyric acid (PBA)] were used to observe the resultant changes in the aforementioned molecules. The results obtained revealed that the overexpression of salusin-α increased the level of AdipoR2 in 293T and HepG2 cells, led to an upregulation of the levels of PPARα and ApoA5, and inhibited the expression of SREBP-1c, whereas the salusin-α interference lentivirus exerted the opposite effects. Notably, thapsigargin inhibited the expression of AdipoR2, PPARα and ApoA5 in HepG2 cells of pHAGE-Salusin-α group, and caused an increase in the level of SREBP-1c, whereas the opposite effects were observed in pLKO.1-shSalusin-α#1 group upon treatment with PBA. Taken together, these data demonstrated that overexpression of salusin-α upregulated AdipoR2, which in turn activated the PPARα/ApoA5/SREBP-1c signaling pathway to inhibit lipid synthesis in HepG2 cells, thereby providing theoretical data on which to base the clinical application of salusin-α as a novel peptide for molecular intervention in fatty liver disease.

Correspondence to: Dr Yuxue Wang, Department of Laboratory Medicine, Hubei University of Chinese Medicine, 16 Huangjiahu West Road, Wuhan, Hubei 430065, P.R. China
E-mail: wangyuxue20012001@163.com

Professor Guofu Gong, Department of Clinical Laboratory, Ezhou Central Hospital, 9 Wenxin Road, Ezhou, Hubei 436000, P.R. China
E-mail: ezggf666666@163.com

*Contributed equally

Key words: salusin-α, adiponectin receptor 2, lentivirus, PPARα/ApoA5/SREBP-1c axis, lipid metabolism

Introduction

Salusin-α and adiponectin are (two) vasoactive peptides associated with atherosclerosis that have been previously discovered. Salusin-α is one of the alternatively spliced products derived from human torsional dystrophin TOR2A mRNA, which was discovered by Shichiri *et al* (1) through the analysis of human DNA library in 2003. It mainly exists in blood vessels, the central nervous system and kidneys, and is a previously identified vasoactive peptide that inhibits atherosclerosis (2). A recent study reported that lipid metabolism disorder is the most important risk factor in the development of atherosclerosis (3), and salusin-α is able to inhibit the synthesis of lipids in macrophages through downregulating acyl-coenzyme A: cholesterol acyltransferase-1 (ACAT-1), thereby inhibiting the process of foam formation of macrophages (4). Furthermore, a previously published clinical study confirmed that the level of salusin-α in serum is increased, whereas the level of triglycerides (TG) is significantly decreased (5). Additionally, it was also reported that, in a study of patients who experienced dyslipidemia due to hemodialysis treatment, salusin-α was negatively correlated with low-density lipoprotein, whereas it was positively correlated with the high-density lipoprotein/low-density lipoprotein cholesterol ratio (6). These results revealed that salusin-α could regulate lipid metabolism, thereby inhibiting atherosclerosis.

Alternatively, adiponectin, an endogenous cytokine, is mainly secreted by adipose tissue, which fulfills its biological role via combining with its receptors (7). At present, there are three known adiponectin receptors, namely adiponectin receptors 1 and 2 (AdipoR1 and AdipoR2) and T-cadherin (8). AdipoR1 is mainly expressed in skeletal muscle, where it is involved in activation of the AMP-activated protein kinase (AMPK) pathway, whereas AdipoR2 is mainly expressed in the liver, and is associated with the activation of peroxisome proliferator-activated receptor-α (PPARα) (9). A recent study suggested that adiponectin could combine with AdipoR1 or AdipoR2 to promote fatty acid oxidation and inhibit lipid synthesis (10). Similar to salusin-α, there is evidence that adiponectin also inhibits the synthesis of lipids and atherosclerosis via binding with receptors to downregulate ACAT-1 (11); moreover, the content of adiponectin in circulating blood is positively correlated with high-density lipoprotein, and negatively correlated with TG (12). The evidence to date has collectively shown that salusin-α and adiponectin are peptides associated with lipid metabolism, and they exert the same biological effects in certain respects. However, to the best of our knowledge, no studies have been published to date concerning whether any association exists between salusin-α and adiponectin.

Fatty liver disease, which is a disease associated with lipid metabolism, is characterized by an excessive accumulation of lipids in hepatocytes due to various different causes (13). In recent years, fatty liver disease has been recognized as one of the main causes of chronic liver disease throughout the world. Indeed, a previously published epidemiological investigation demonstrated that its prevalence has reached 25% worldwide, and the incidence rate is starting to increase in younger populations (14). Simple fatty liver disease can develop into steatohepatitis, liver fibrosis, and even cirrhosis and liver cancer, in addition to inducing certain cardiovascular diseases, including atherosclerosis (15). However, if diagnosed sufficiently early, fatty liver disease is reversible, and early diagnosis and treatment can cause the condition to return to normal (16). Therefore, it is very important to investigate how to inhibit the synthesis and accumulation of lipids in the hepatocytes of patients with fatty liver, with the aim of reducing the incidence rate of fatty liver disease. Numerous studies have been conducted which have shown that adiponectin binds to AdipoR2 and activates PPARα, subsequently directly affecting lipid synthesis in liver cells through the apolipoprotein A5 (ApoA5)/sterol regulatory element-binding transcription factor 1 (SREBP-1c) signaling pathway (17,18). Tang *et al* (19) proposed that, compared with a high-fat diet model group, the levels of fatty acid synthase and acetyl-CoA carboxylase-α were significantly reduced in the liver tissue of mice following salusin-α treatment, and the expression levels of PPARα, carnitine palmitoyltransferase 1A and cytochrome P450 7A1 were also significantly increased, thereby promoting the oxidation of fatty acids and decomposition of cholesterol, inhibiting fatty liver. Clearly, salusin-α and adiponectin can exert the same effects on lipid metabolism; however, it remains unclear whether salusin-α is able to effect changes in the downstream signal molecules of hepatocytes through AdipoR2. Based on the observations that salusin-α and adiponectin exert numerous similar biological effects, and can both effect changes in the level of the downstream molecule PPARα, it was hypothesized that salusin-α may regulate changes in downstream signaling molecules via AdipoR2. However, to the best of our knowledge, few studies have been undertaken on the correlation between salusin-α and AdipoR2.

Consequently, in the present study, 293T cells were first infected with synthesized overexpression and interfering salusin-α lentiviruses, and then changes in the level of AdipoR2 were detected using semi-quantitative (SQ)-PCR. Subsequently, HepG2 cells were also infected using the identical method, and the AdipoR2 level was assessed. Western blot (WB) analysis was then employed to detect whether salusin-α could regulate the PPARα/ApoA5/SREBP-1c signaling pathway in liver cells through AdipoR2. In order to further confirm that salusin-α exerts a role through AdipoR2, an agonist and inhibitor of AdipoR2 were also used to investigate the regulation of lipid synthesis mediated by salusin-α in HepG2 cells via the PPARαApoA5/SREBP-1c signaling pathway. Collectively, the findings of the present study provided a theoretical and experimental basis for exploring the potential mechanism via which salusin-α inhibits fatty liver.

Materials and methods

Construction of recombinant plasmids. According to the human TOR2A gene sequence number (NM-001134430), the sequence of salusin-α was determined, and a short hairpin (sh)RNA design tool (BLOCK-iT™ RNAi Designer; Thermo Fisher Scientific, Inc.) was used to design three salusin-α interference sequences (Table I). The specificity of these sequences was then confirmed through BLAST analysis on NCBI database. These sequences were synthesized by Sangon Biotech Co., Ltd. Transfer plasmids [pHAGE (cat. no. 118692) and pLKO.1 (cat. no. 8453; both from Addgene)] and auxiliary plasmids [psPAX2 (cat. no. 12260) and pMD2G (cat. no. 12259; both from Addgene)] were provided by Tongji Medical College of Huazhong University of Science and Technology. SnapGene-designed salusin-α primers contained *Bam*HI (cat. no. 1010A) and *Xho*I (cat no. 1094A; both from Takara Biotechnology Co., Ltd.) restriction sites (Table II), and pHAGE-Salusin-α was constructed according to the method of double-enzyme-digestion molecular cloning. Briefly, the PCR amplification product containing salusin-α and pHAGE vector were digested with *Bam*HI and *Xho*I to produce the same sticky ends. Subsequently, the salusin-α gene sequence and linear Phage vector were purified and then joined using T4 DNA ligase (cat no. 2011A; Takara Biotechnology Co., Ltd.) in an overnight incubation at 16˚C. pLKO.1-shSalusin-α was constructed according to the construction method for interference plasmids. The two synthesized interference sequences were annealed to form a double-stranded DNA, which was then ligated with the line vector of pLKO.1 that had been digested by *Age*I (cat. no. R3552S; New England BioLabs, Inc.) and *Eco*RI (cat. no. R3101V; New England BioLabs, Inc.). The constructed pHAGE-Salusin-α and pLKO.1-shSalusin-α plasmids were respectively transfected into TOP10 competent cells. The transfection mixture was coated onto an LB plate and cultured overnight at 37˚C in an incubator, prior to the selection of colonies on the plate. The constructed plasmids were confirmed by colony PCR. Table II shows the salusin-α primers and

Table I. Synthetic interfering sequences of salusin-α. A total of 3 interference sequences are included, all of which were used to construct pLKO.1-shSalusin-α. Target site: shSalusin-α specifically designed for this sequence of salusin-α. The bold part is the sense chain and the antisense chain, the antisense chain is the reverse repeat sequence of the sense chain, the 'CTCGAG' is loop.

Name	Sequences (5'→3')	Target site (bp)
shSalusin-α#1	Sense: CCGG**GCCCTTCCTCCCGCTCCAGCG**CTC GAG**CGCTGGAGCGGGAGGAAGGGC**TTTTTG Antisense: AATTCAAAAA**GCCCTTCCTCCCGCTC CAGCG**CTCGAG**CGCTGGAGCGGGAGGAAGGGC**	7-27
shSalusin-α#2	Sense: CCGG**GCGGCACCACGTCCGGCACTG**CTC GAG**CAGTGCCGGACGTGGTGCCGC**TTTTTG Antisense: AATTCAAAAA**GCGGCACCACGTCCGG CACTG**CTCGAG**CAGTGCCGGACGTGGTGCCGC**	25-45
shSalusin-α#3	Sense: **T**CTCGAG**AGCTCGTTGAGCACGCAGTC** TTTTTG Antisense: AATTCAAAAA**GCACTGCGTGCTCAACG AGCT**CTCGAG**AGCTCGTTGAGCACGCAGTGC**	40-60

Sh-, short hairpin.

Table II. pSequences of primers used for semi-quantitative PCR. shSalusin-α#1-3: interference sequences of salusin-α#1, 2 and 3; the text highlighted in bold represents the restriction site; because the forward primer was designed on the pLKO.1, the interference sequences shSalusin-α#1-3 share a forward primer.

Gene name	Sequence (5'→3')	Length (bp)
WPRE	F: CGCTATGTGGATACGCTGCTTTA	93
	R: GCAACCAGGATTTATACAAGGAGGA	
GAPDH	F: GTCTCCTCTGACTTCAACAGCG	131
	R: ACCACCCTGTTGCTGTAGCCAA	
Salusin-α	F: CA**GGATCC**AGTGGTGCCCTTCCTCCCG	101
	R: CAT**CTCGAG**CTTGGCTCCAGGCCCAGC	
AdipoR2	F: AGGACTCCAGAGCCAGATATAAG	273
	R: CCACCGCCCTTCCCATACC	
shSalusin-α#1-3	F: CGAGACTAGCCTCGAGCGGCC	
shSalusin-α#1	R: CTCGAGCGCTGGAGCGGGA	311
shSalusin-α#2	R: CTCGAGCAGTGCCGGACGT	311
shSalusin-α#3	R: CTCGAGAGCTCGTTGAGCACGC	311

AdipoR2, adiponectin receptor 2; F, forward; R, reverse; WPRE, woodchuck hepatitis virus post-transcriptional regulatory element.

the primers designed for the interference sequence. Positive colonies of successfully cloned plasmid were inoculated into LB culture medium. Precisely following the instructions of the plasmid extraction kit (cat. no. 9760; Takara Biotechnology Co., Ltd.), the recombinant plasmids were extracted from the bacterial solution and sent to Sangon Biotech Co., Ltd. for sequencing. Finally, the recombinant plasmids were amplified and purified, and a large number of highly purified plasmids were obtained for subsequent experiments.

Cell culture and packaging of lentivirus. 293T cells (cat. no. CRL-3216TM; American Type Culture Collection), which are also called human embryonic kidney cells (an epithelial-like cell that was isolated from the kidney of a patient), were obtained from the Tongji Medical College of Huazhong University of Science and Technology. The HepG2 cell line (has an epithelioid morphology and was isolated from male liver cancer) was purchased from ENOVA BIO (www.enovabio.com; cat. no. ECL0103). After STR identification, the aforementioned HepG2 cell line was found to have a similarity rate and of 98.51% with the HepG2 cell line in CELLOSAURUS database (accession no. CVCL_0027). Both cell lines were maintained in high-glucose DMEM (cat. no. PM150210; Procell Life Science & Technology Co., Ltd.) containing 10% (v/v) fetal bovine serum, 100 U/ml penicillin and 100 μg/ml streptomycin (cat. no. MA0110; Dalian Meilun

Biology Technology Co., Ltd.) in a humidified incubator containing 5% CO_2 at 37˚C. Mycoplasma detection was performed on the cells before the experiment, and HepG2 cells were identified by STR profiling to determine that there was no cross-contamination of the cells. To explore the manner in which salusin-α may regulate the PPARα/ApoA5/SREBP-1c pathway through AdipoR2, after having infected HepG2 cells with the lentivirus for 24 h, the cells were coincubated with Complete™ medium containing either the AdipoR2 inhibitor (1 μM thapsigargin; cat. no. T9033; MilliporeSigma) or the AdipoR2 agonist [20 μM 4-phenyl butyric acid (PBA); cat. no. 2312-73-4; Sigma-Aldrich; Merck KGaA] for 24 h (20).

293T cells in the exponential growth phase were selected for packaging of lentivirus. In this experiment, the second-generation lentivirus was packaged by liposome transfection. According to the Simple-Fect Transfection Reagent (cat. no. profect-01; Wuhan Signal Shuguang Biotechnology Co., Ltd.), 4 μg recombinant plasmid (pHAGE-Salusin-α or pLKO.1-shSalusin-α#1-3), 3 μg pMD2G plasmid and 1 μg psPAX2 plasmid were co-transfected into 293T cells to package lentivirus. The transfected 293T cells were placed into the 5%-CO_2 incubator at 37˚C for culture. After 24 h of transfection, the culture medium was changed, and then continued to be cultured at 37˚C. The peak period for 293T cells to produce lentivirus is 48-72 h after transfection; therefore, the cell supernatant was collected at 48 and 72 h respectively, and the cytopathic effect (CPE) was observed under an inverted optical microscope. After 72 h of transfection, the ability of cells to produce lentivirus rapidly decreased and a large number of cells died due to CPE, at which time, the culture could be terminated. The collected cell supernatants were centrifuged at 4˚C, 1,500 x g for 10 min to remove the cell residue, subsequently filtered with 0.45 μm filter, sub-packaged and stored at -80˚C for future experiments. In addition, 500 μl of the aforementioned filtered cell supernatant was collected, and the viral RNA was extracted using the TRIzol™ method (cat. no. 9108; Takara Biotechnology Co., Ltd.). Given that the pHAGE/pHAGE-Salusin-α and shMock/pLKO.1-shSalusin-α plasmids carried the specific genes woodchuck hepatitis virus post-transcriptional regulatory element (WPRE) and shSalusin-α respectively, the existence of WPRE and shSalusin-α was confirmed using semi-quantitative (SQ)-PCR (Table II) and 1.5% agarose gel electrophoresis (GoldView) to verify the production of this virus.

Preparation of transmission electron microscopy (TEM) specimens. After 72 h of culture, precooled 2.5% glutaraldehyde (cat no. G916054; Shanghai Macklin Biochemical Co., Ltd.) was directly added to the 293T cells used for packaging without rinsing, and the cells were fixed for 1 h. The cells were quickly scooped out with a cell shovel and transferred to a centrifuge tube. Most of the cellular supernatant was removed by centrifugation at 4˚C, 300 x g for 5 min, leaving ~1 ml of residual supernatant for gently blowing apart the cells, and then transferred to 1.5-ml EP tubes. After standing vertically and allowing the cells to settle naturally for 1 h, the supernatant was gently discarded, and 1 ml newly precooled 2.5% glutaraldehyde was slowly added along the tube wall. The cells were then stored in a refrigerator at 4˚C for 2 h, 1% osmic acid fixed at 4˚C for 2 h. Buffer washing and dehydration of 50% pyruvic acid for 15 min was performed. Epon 812 (cat no. 02662-AB; Structure Probe, Inc.) was used as a resin embedding agent to embed the sample at 60˚C for 36 h, and then a slicer was used to cut the sample into 50 nm. Subsequently, at room temperature, the sample was dyed with uranium acetate for 30 min, then with lead citrate for 15 min, and finally sent to the People's Hospital of Wuhan University for subsequent TEM experiments.

Table III. Real-time fluorescence quantitative PCR system.

Components	Volume (μl)
Ultra-pure water	7.2
2X SYBR Mix	10
Upstream primer (10 μM)	0.4
Downstream primer (10 μM)	0.4
Template	2
Total volume	20

Determination of lentivirus titer and MOI. 293T cells were inoculated into 12-well plates for $2x10^5$ cells per well, and cultured overnight at 37˚C. On the second day, the cells proliferated to 20-30% fusion density, and the viral solution stored in the refrigerator at -80˚C was melted in the ice bath, and the cell culture solution containing DMEM (without serum) was used for gradient dilution as follows: i) First diluent: 10 μl virus solution + 90 μl culture medium for virus dilution; ii) Second diluent: 10 μl of first diluent + 90 μl culture medium for virus dilution; iii) Third diluent: 10 μl of second diluent + 90 μl culture medium for virus dilution; iiii) Fourth diluent: 10 μl of third diluent + 90 μl culture medium for virus dilution. The desired cell hole was selected, the lentivirus diluent in each tube was gently mixed, 90 μl was added into each cell hole, and placed into a cell incubator at 37˚C for overnight culture. The control virus with known titer was added with No. 1-4 diluent, and the sample to be tested was added with first and second diluent. On the fifth day, the cell state was observed, the cell density was >80%, and RNA was extracted for reverse transcription-quantitative PCR (RT-qPCR). After the lentivirus infected cells successfully, 500 μl TRIzol solution was added to each well of 12-well plate to extract the total RNA. After that, RT-qPCR were used to detect the target gene WPRE and internal reference gene GAPDH (primer sequences are listed in the Table II). PCR system is presented in Table III. The thermocycling conditions for the PCR program were as follows: 95˚C pre-denaturation for 30 sec; denaturation at 95˚C for 15 sec; annealing at 60˚C for 60 sec; 40 cycles. Finally, the standard curve was constructed based on the CT value of WPRE and GAPDH in the control group and the known virus titer, and then the relative virus titer was calculated according to the CT value of the experimental group. The virus titer equals to: The relative virus titer x dilution multiple.

Multiple data have shown that the MOI of HepG2 is 5-10, thus the six MOI gradients of 2, 5, 7, 10, 15 and 20 were set. Cells in each well of the six-well plate were inoculated at a density of $8x10^5$. When the density reached 80% the following day (the number of cells was ~$2x10^6$), according

to the formula MOI=(virus titer x added virus volume)/the number of cells transfected, the corresponding added virus volumes were calculated to be 0.2, 0.5, 0.7, 1, 1.5 and 2 ml respectively. Lentivirus was added one by one, and the fresh culture medium was changed after 12 h. Antibiotics were used for screening and puromycin (cat no. ST551; Beyotime Institute of Biotechnology) was diluted to 100 μg/ml (from an initial concentration of 10 mg/ml). Then, according to the manufacturer's instructions, puromycin was used at a concentration of 3 μg/ml for HepG2 cells and 2 μg/ml for 293T cells (60 μl of diluted puromycin was added to the six-well plate (2 ml) of HepG2 and 40 μl of diluted puromycin to the six-well plate (2 ml) of 293T cells]. After 3-5 days of culture, under the microscope, it was found that the pore cells with 1 ml of virus had a higher survival rate and favorable cell state, and the pores with >1 ml of virus had different degrees of black spots, thus the appropriate MOI value of HepG2 was 10. MOI value of 293T cells was 1.

Lentiviral infection. Before the formal experiment, the collected pHAGE, shMock and pLKO.1 lentiviruses were used to infect the cultured 293T cells respectively. At the same time, a group of 293T cells without virus (NC group) was set up, and the expression of salusin-α in each control group was detected at 48 h after infection. After that, the formal experiment began. 293T cells in favorable growth condition were inoculated in sixwell plates at a density of $1.2x10^5$ cells/well. The next day, after the cell confluence reached 70%, lentivirus infection was initiated. According to the titer and MOI detected by the aforementioned experiments, it was detected that 1 ml of viral stock solution was the most favorable. Therefore, after the medium in the six-well plate had been removed, 1 ml of the aforementioned viral solution and 1 ml fresh complete medium were added to each well, in addition to polybrene (cat no. BL628A; Biosharp Life Sciences) at a final concentration of 8 μg/ml in each well. Subsequently, the six-well plate was placed into the 5%-CO_2 incubator at 37˚C for culture overnight. After 12 h incubation, the medium was replaced with fresh culture medium. Transiently infected 293T cells were collected 24 h after infection, and RT-qPCR (Table II) and WB analyses were then used to analyze the expression level changes of the target genes and proteins. The identical method of lentiviral infection was used for the HepG2 cells as for the 293T cells, with the only difference that, whereas 293T cells are easily infected and changes in gene and protein expression can be detected after only 24 h of infection, for the HepG2 cells the rapid collection of infected cells 48 h after infection to detect changes in target proteins via WB analysis was required. Moreover, based on the aforementioned experimental procedures, in order to explore the manner in which salusin-α may regulate the PPARα/ApoA5/SREBP-1c pathway through AdipoR2, after having infected HepG2 cells with the lentivirus for 24 h, the agonist (PBA) and inhibitor (thapsigargin) of AdipoR2 were respectively added, then the expression levels of proteins associated with lipid metabolism were detected.

SQ-PCR analysis. The core of SQ-PCR is to determine the number of cycles of the target gene at the exponential amplification period. In order to determine the number of SQ-PCR cycles of the target gene, total RNA was extracted from 293T cells that had not been transfected with the virus using TRIzol™ (cat no. 9108; Takara Biotechnology Co., Ltd.), and following the instructions of the reverse transcription kit (cat no. D7170M; Beyotime Institute of Biotechnology), 1 μg template RNA was reverse-transcribed into cDNA. PCR Thermocycler (Biometra Tone 96 G; Analytik Jena AG) was used to PCR-amplify salusin-α (Table II) for multiple rounds, and the PCR cycle numbers were set to 20, 22, 24, 26, 28, 30 and 32, respectively. The thermocycling conditions for PCR were as follows: 94˚C pre-denaturation for 3 min; denaturation at 94˚C for 30 sec; annealing at 64˚C for 30 sec; and extension at 72˚C for 30 sec, completed the cycle number of times, and extended for 5 min at the end. The method used to find the number of cycles used for AdipoR2 SQ-PCR was consistent with that for salusin-α, except that the annealing temperature for AdipoR2 was set at 60˚C. Subsequently, the PCR products were electrophoresed (1.5% agarose gels), and the electrophoretic bands were analyzed using Tanon 1600 Gel Imaging System (Tanon Science and Technology Co., Ltd.) to determine the index stage and platform stage of PCR amplification. Subsequently, PCR was performed for the target gene with the number of cycles at the exponential stage, and the same number of cycles of PCR was used for GAPDH (Table II) as the internal control to eliminate any error caused by sample addition. Finally, agarose electrophoresis with subsequent imaging in the gel image system was performed. The brightness of the bands was observed, and the optical density (OD) of each group of bands was measured using the Tianneng gel analysis software (biotanon.com). The ratios of the target gene OD value/GAPDH OD value were used to express the relative expression level of mRNA, to compare the expression levels of the target genes in each group.

WB analysis. Control and treatment cells were washed with PBS. After the cells were lysed on ice with RIPA lysate (cat. no. MA0151; Dalian Meilun Biology Technology Co., Ltd.) containing PMSF (cat. no. G2008-1ML; Wuhan Servicebio Technology Co., Ltd.) for 30 min, the cells in each group were respectively collected, and centrifuged at 4˚C (4,500 x g for 10 min) to remove the cell fragments. Subsequently, the total protein concentration in the supernatant was measured using a bicinchoninic acid (BCA) kit (cat no. E-BC-K318-M; Elabscience Biotechnology, Inc.), and the protein content of each sample was adjusted to the same concentration at 5 μg/μl with PBS. The diluted protein samples were then mixed with 1X SDS loading buffer solution and denatured at 95˚C for 5 min, and SDS-PAGE (either 8 or 10% gels) was used to separate the proteins, which were subsequently transferred to PVDF membranes (cat no. IPVH00010l; EMD Millipore). Non-specific binding to the membranes was blocked with 5% skimmed milk powder (cat no. 1172GR100; BioFRoxx; neoFroxx) for 2 h at room temperature, and the membranes were subsequently incubated overnight at 4˚C with different primary antibodies, as follows: Anti-salusin-α rabbit polyclonal antibodies (1:1,000; cat. no. ab232928; Abcam), anti-AdipoR2 mouse monoclonal antibodies (1:1,000; cat. no. sc-514045; Santa Cruz Biotechnology, Inc.), anti-PPARα rabbit polyclonal antibodies (1:1,000; cat. no. ab227074; Abcam), anti-ApoA5 mouse monoclonal antibodies (1:1,000; cat. no. ab115772;

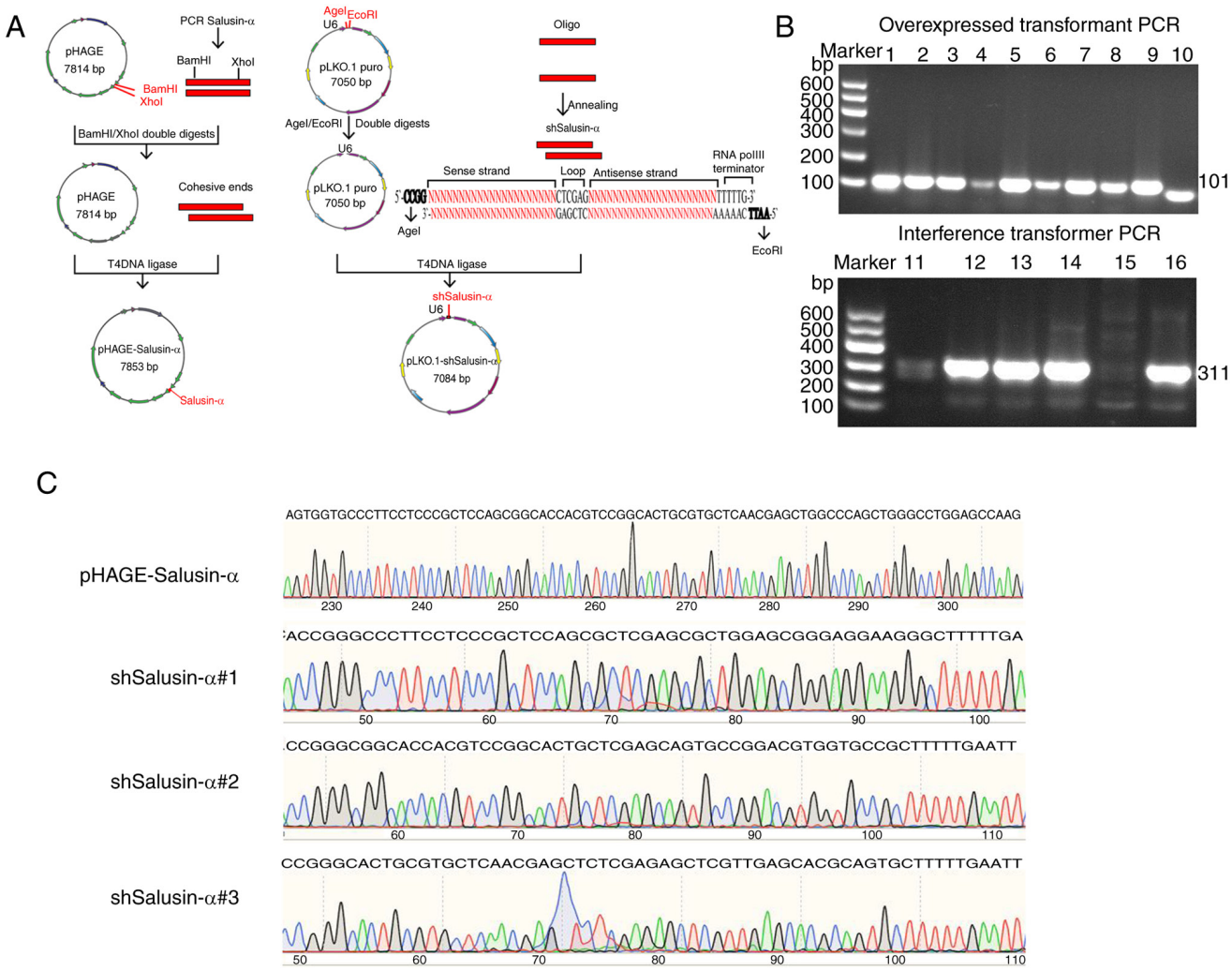

Figure 1. Construction and identification of recombinant plasmid. (A) Schematic diagram of construction of the recombinant plasmids pHAGE-Salusin-α and pLKO.1-shSalusin-α#1-3. (B) The recombinant plasmids of pHAGE-Salusin-α and pLKO.1-shSalusin-α#1-3 were identified by colony PCR. Numbers 1-10 were the selected monoclonal colonies of pHAGE-Salusin-α, in which 1-9 were positive clones; 11-16 is the selected monoclonal colony of pLKO.1-shSalusin-α#1-3 (specifically, pLKO.1-shSalusin-α#1: 11 and 12; pLKO.1-shSalusin-α#2: 13 and 14; and pLKO.1-shSalusin-α#3, 15 and 16), of which 12-14 and 16 were positive clones. (C) Recombinant plasmid DNA sequencing map (partial results) are shown, the inserted sequence was consistent with the sequence of salusin-α and designed shSalusin-α#1-3. shSalusin-α#1-3, pLKO.1-shSalusin-α#1-3 represent interference salusin-α; pHAGE-Salusin-α represents overexpression salusin-α; sh-, short hairpin.

Abcam), anti-SREBP-1c rabbit polyclonal antibodies (1:1,000; cat. no. ab28481, Abcam) and anti-GAPDH rabbit polyclonal antibodies (1:10,000; cat. no. ab9485; Abcam). Subsequently, diluted horseradish peroxide-labeled secondary antibodies were added as follows: Goat anti-rabbit IgG (1:50,000; cat. no. ab205718; Abcam) and goat anti-mouse IgG (1:10,000; cat. no. ab205719; Abcam). The membranes were incubated on a shaking table at room temperature for 2 h, prior to washing three times using TBST (0.1% Tween). WBs were visualized using ECL chemiluminescence kit (cat. no. MA0186; Dalian Meilun Biology Technology Co., Ltd.), and a chemiluminescence imaging system was used for exposure imaging. Furthermore, the gray values of the strips were analyzed with ImageJ (V1.8.0.112; National Institutes of Health), and the gray value ratios of each group of target strips and internal reference strips were recorded.

Statistical analysis. All data are expressed as the mean ± standard deviation. The statistical analysis was conducted using GraphPad Prism 8 (Dotmatics). All experiments were performed three times. Prior to the statistical analysis, the normality of data was examined using the Shapiro-Wilk test. ANOVA was used for normally distributed data, whereas the Kruskal-Wallis H rank sum test was used for non-normally distributed data. Depending on the design of the experiment, the data were analyzed using one-way ANOVA followed by Tukey's post hoc test. $P<0.05$ was considered to indicate a statistically significant difference.

Results

Construction and identification of recombinant plasmid. The construction process for the recombinant plasmid is revealed in Fig. 1A. Positive clones of the TOP10 *E. coli* competent cells transfected with the recombinant plasmids pHAGE-Salusin-α and pLKO.1-shSalusin-α were selected. The electrophoretic results of the colony PCR products revealed that there were bands at ~100 and 300 bp, respectively (Fig. 1B), which was

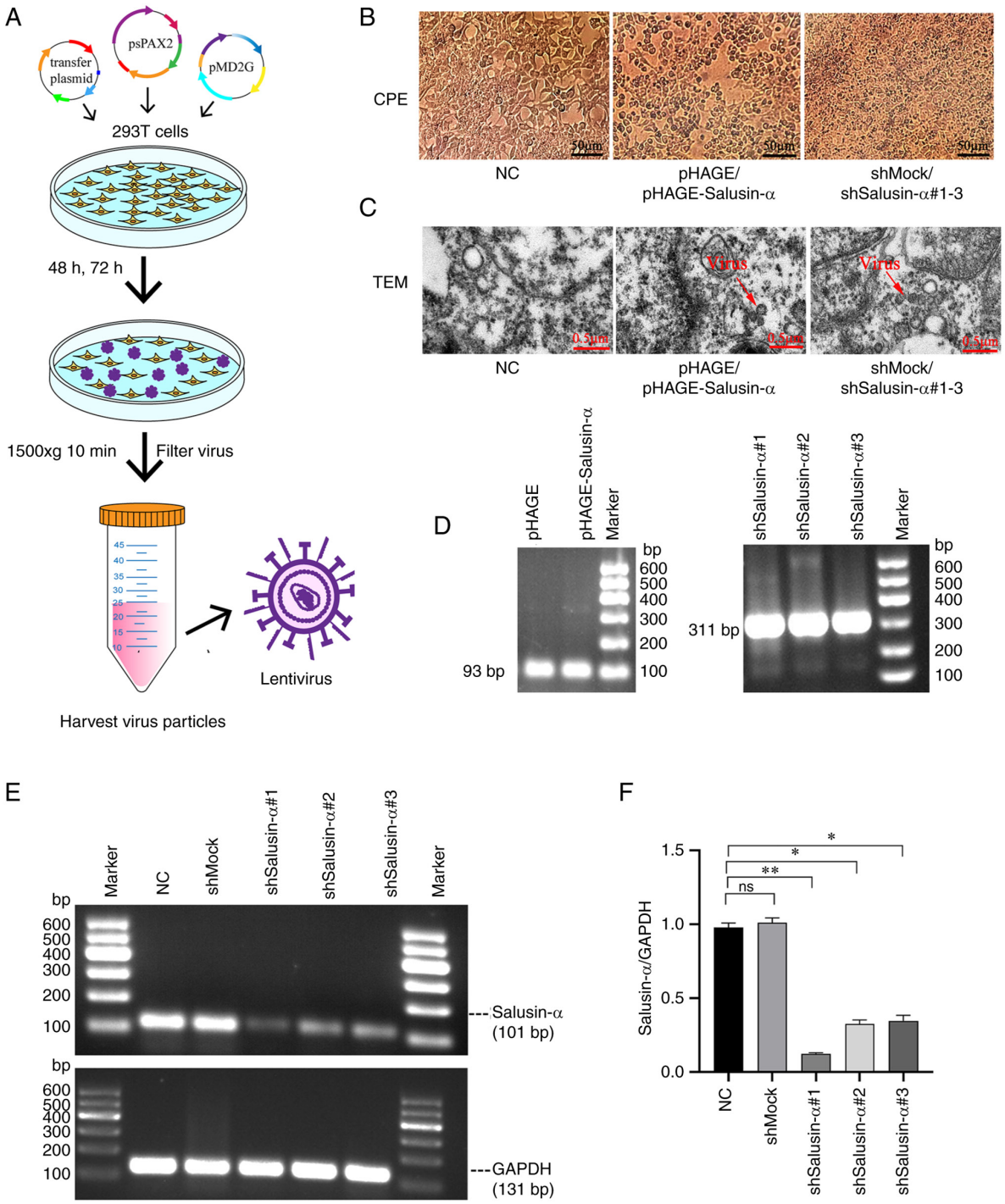

Figure 2. Generation and verification of lentivirus, and the selection of the interference sequence. (A) Schematic diagram of the lentivirus packaging process. (B) After 48 h of plasmid transfection, 293T cells in the pHAGE, pHAGE-Salusin-α, shMock and shSalusin-α#1-3 groups exhibited CPE, whereas the NC group grew normally without CPE. Scale bar, 50 μm. (C) After 72 h of plasmid transfection, TEM of 293T cells was performed for each group. The red arrows indicate the lentiviral particle. No viral particles were observed in the NC group. Scale bar, 0.5 μm. (D) Graphs of the electrophoretic results after RNA extraction, reverse transcription and then PCR from each group of viral fluids. Sizes of 93 and 311 bp for identified for WPRE and the shSalusin-α#1-3 sequences, respectively. It should be noted that WPRE is a post-transcriptional regulatory sequence on the pHAGE plasmid; 293T cells do not contain this sequence. (E) The interference effect of pLKO.1-shSalusin-α#1, 2 and 3 was analyzed by semi-quantitative PCR, and the sequence with the best interference effect was selected for subsequent experiments by comparing the ratio of salusin-α/GAPDH. (F) The relative expression levels of salusin-α gene in 293T cells for each group are shown. Data are presented as the mean ± SD. *P<0.05 and **P<0.01 by t-test; ns, no significant difference; NC, negative control; 'shMock' is a meaningless RNA used as a control for shSalusin-α; shSalusin-α#1-3, pLKO.1-shSalusin-α#1-3 represent interference salusin-α; pHAGE-Salusin-α represents overexpression salusin-α; CPE, cytopathic effect; TEM, transmission electron microscopy; WPRE, woodchuck hepatitis virus post-transcriptional regulatory element; sh-, short hairpin.

consistent with the anticipated molecular weights of 101 bp for salusin-α and 311 bp for shSalusin-α. Subsequently, the sequencing results of the recombinant plasmids were submitted for BLAST analysis on NCBI. These data showed that the inserted DNA sequences of the recombinant plasmids pHAGE-Salusin-α and pLKO.1-shSalusin-α were completely

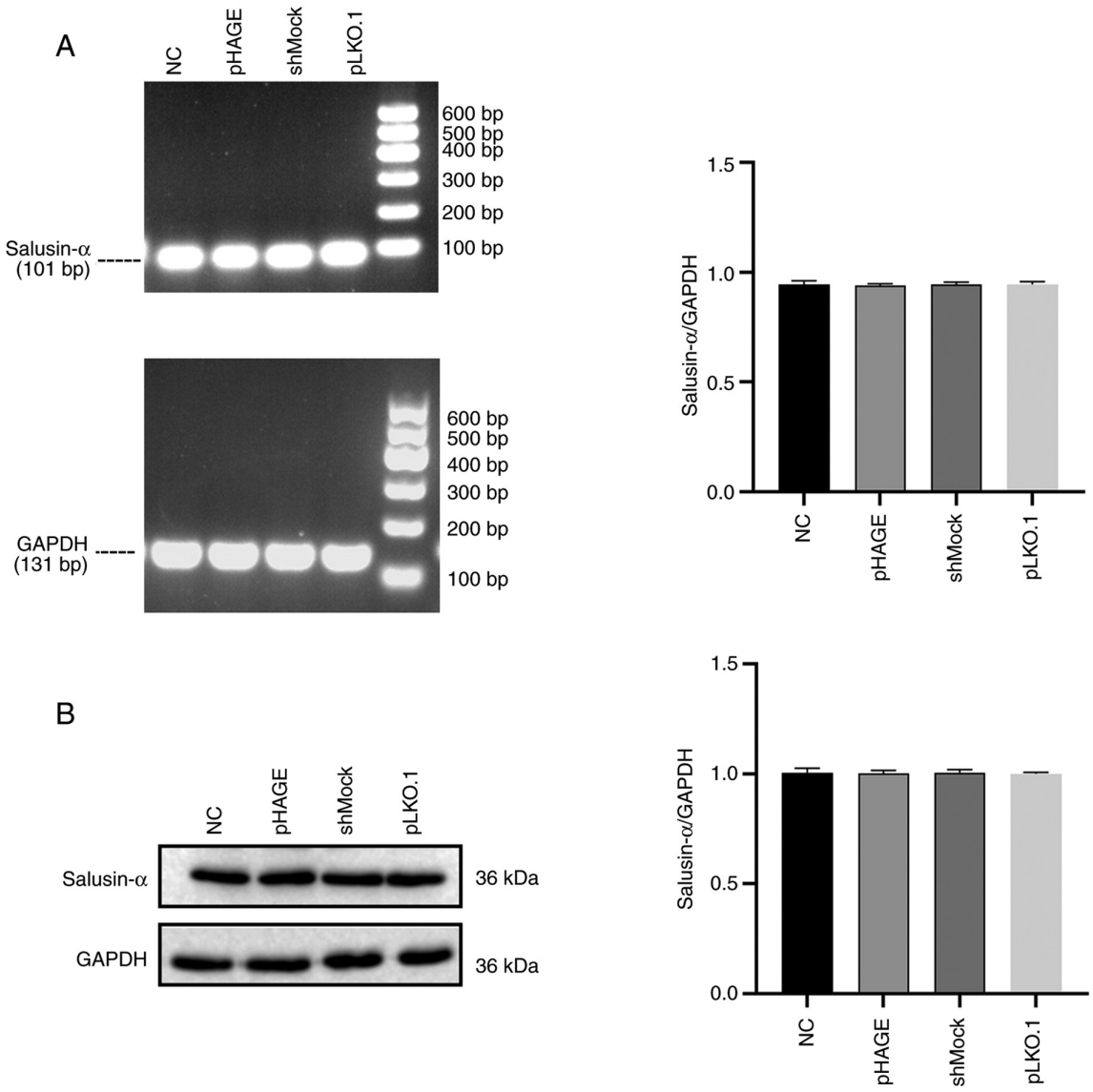

Figure 3. The expression of salusin-α in 293T cells in each control group. (A) Expression of salusin-α mRNA in 293T cells of each control group, no significant difference (all P>0.05). (B) Expression of salusin-α protein in 293T cells of each control group, no significant difference (all P>0.05); sh-, short hairpin; NC, negative control.

consistent with salusin-α and the designed shSalusin-α#1-3, respectively (Fig. 1C), indicating that the shRNA of salusin-α and salusin-α were accurately inserted into the vectors, and the recombinant plasmids were successfully constructed.

Identification of the lentivirus and selection of interfering sequences. pHAGE-Salusin-α and shSalusin-α recombinant plasmids were co-transfected with the helper plasmids psPAX2 and pMD2G, respectively, into 70% confluent 293T cells to complete the packaging of the lentivirus (Fig. 2A). The peak period of packaging and releasing the virus was 48-72 h after transfection. During this period, it was observed that the 293T cells used to package the lentivirus appeared to clearly exhibit the CPE, whereas the CPE did not appear in the cells of the negative control (NC) group (Fig. 2B), indicating that the packaging of the virus was successful. Similarly, the TEM photos confirmed that lentivirus particles could be observed in the pHAGE, pHAGE-Salusin-α, shMock and pLKO.1-shSalusin-α#1-3 groups, but they were not observed in the NC group (Fig. 2C). Furthermore, according to the PCR electrophoretic results, there were bands at ~100 and 300 bp respectively, which were consistent with the expected sizes of 93 and 311 bp for salusin-α and shSalusin-α respectively, suggesting that the lentivirus packaging was successful (Fig. 2D).

PCR products with the PCR cycle numbers 20-32 were detected via electrophoresis. When the cycle number was 22, the band of salusin-α began to appear, although after cycle numbers 30 and 32, the brightness of the band did not change (data not shown), indicating that this was the beginning of the plateauing-out period. Based on these results, 28 cycles were selected as the number of cycles of SQ-PCR in these experiments for salusin-α. With the same analytical method, the results revealed that, for AdipoR2, 26 was selected as the number of cycles of SQ-PCR (data not shown). Subsequently, 293T cells were infected with the synthetic shMock and pLKO.1-shSalusin-α#1-3 viruses. After 24 h, SQ-PCR was used to detect gene expression and to evaluate the interference efficiency of pLKO.1-shSalusin-α#1-3. In the present study, the electrophoretic band brightness of salusin-α in the

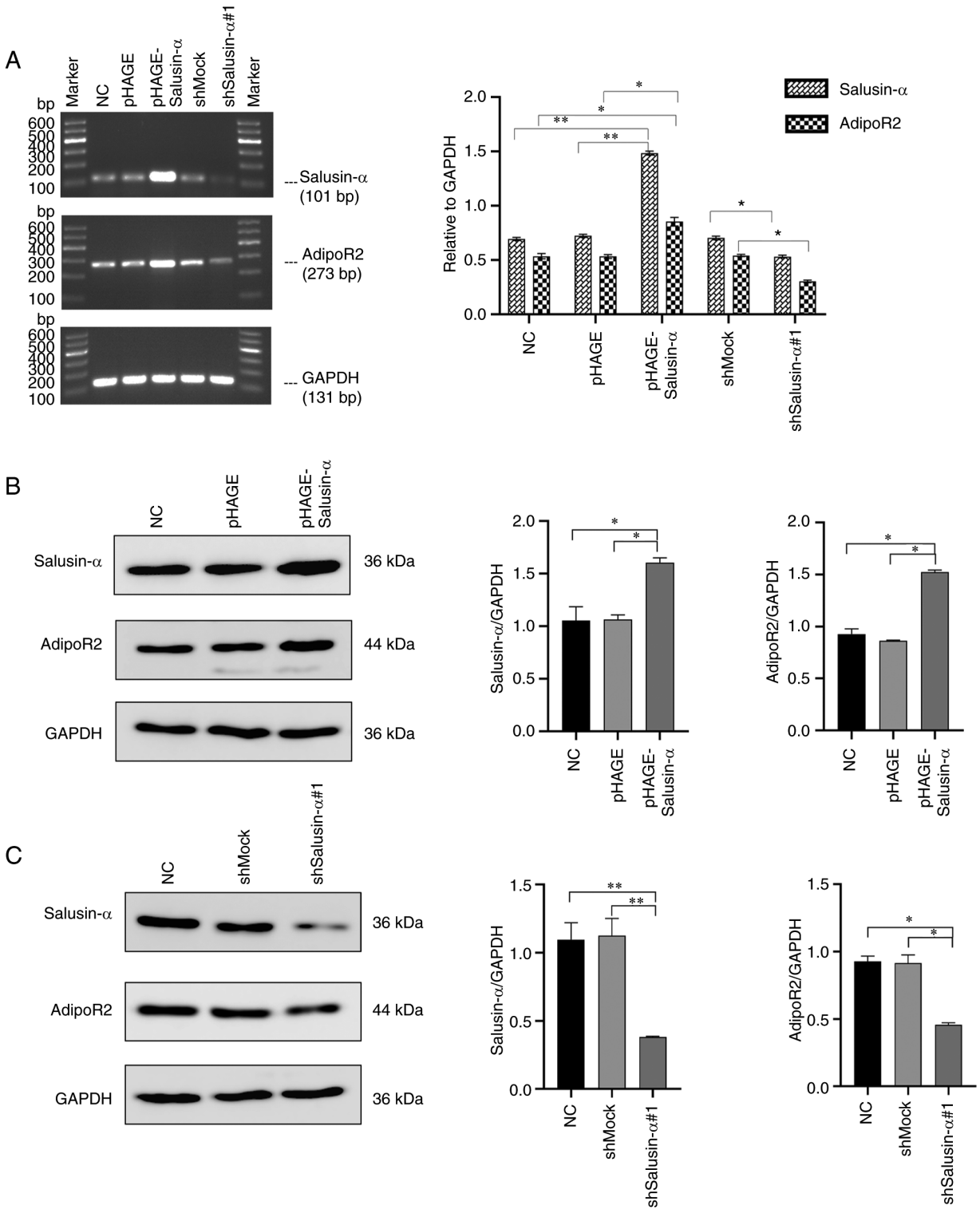

Figure 4. Overexpression or interference of Salusin-α in 293T cells upregulates or inhibits the expression of AdipoR2. (A) After infecting the cells with lentivirus for 24 h, the relative expression levels of salusin-α and AdipoR2mRNA in the 293T cells of each group were detected by semi-quantitative PCR. (B) After infection with overexpression salusin-α lentivirus for 24 h, WB was used to detect the relative expression level of salusin-α and AdipoR2 protein in 293T cells of each group. Data are shown as the mean ± SD. (C) After infection with interference salusin-α lentivirus for 24 h, WB was used to detect the relative expression level of salusin-α and AdipoR2 protein in 293T cells of each group. Data are presented as the mean ± SD. *P<0.05 and **P<0.01 by t-test. AdipoR2, adiponectin receptor 2; WB, western blotting; NC, negative control; shMock, a meaningless RNA as a control for shSalusin-α; shSalusin-α#1, pLKO.1-shSalusin-α#1, representing interference salusin-α; pHAGE-Salusin-α, represents overexpression salusin-α; sh-, short hairpin.

pLKO.1-shSalusin-α#1, 2 and 3 groups was lower compared with that in the shMock and NC groups, indicating that the designed three interfering sequences could all inhibit the expression of the salusin-α gene, but under the same treatment conditions, compared with the NC and shMock groups, the mRNA level of salusin-α in the 293T cells decreased most significantly in the pLKO.1-shSalusin-α#1 group (P<0.05) (Fig. 2E and F). Therefore, the pLKO.1-shSalusin-α#1 group

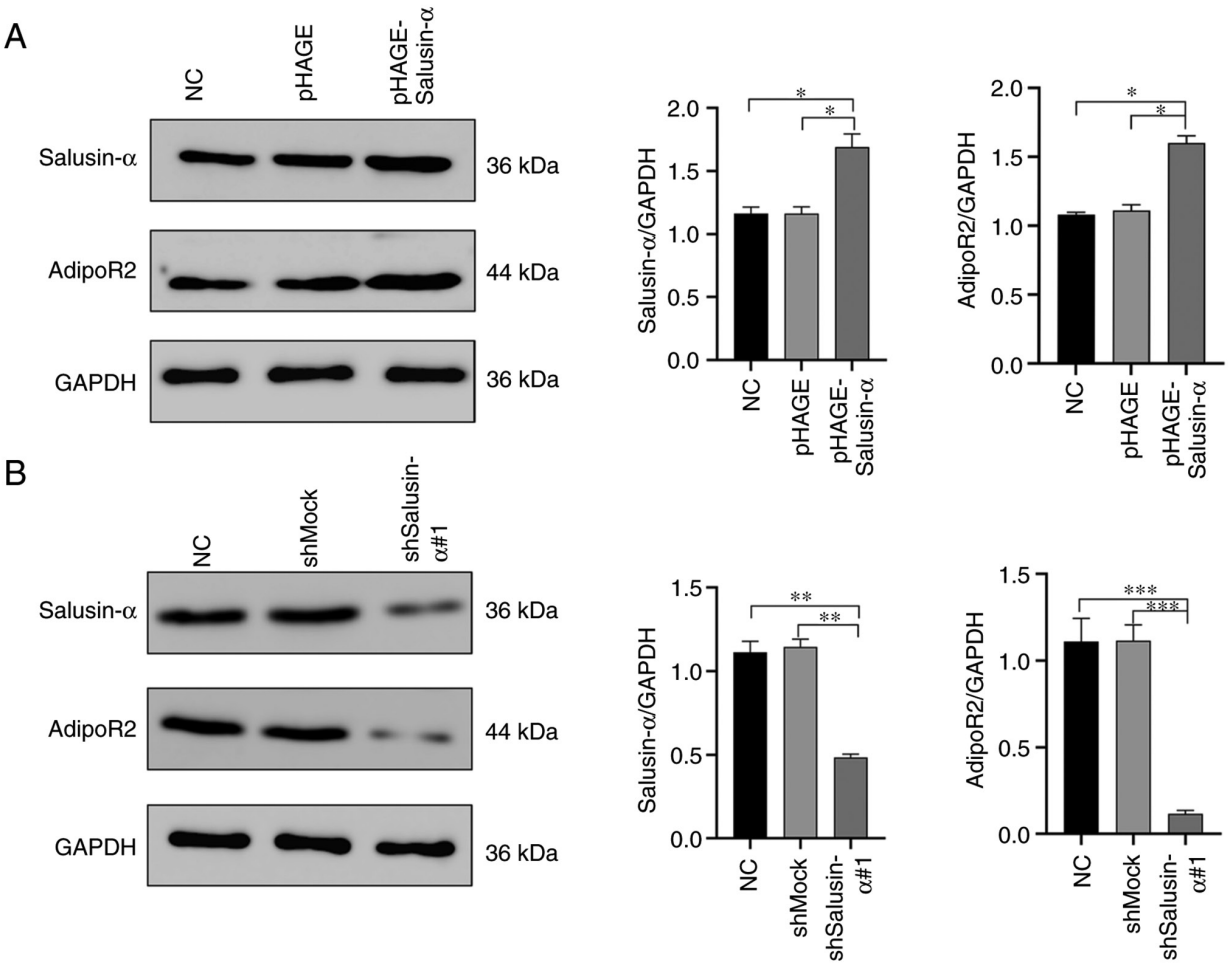

Figure 5. Overexpression or interference of Salusin-α upregulates or inhibits AdipoR2 protein expression in HepG2 cells. After infection with lentivirus for 48 h. (A) The expression of salusin-α and AdipoR2 protein in HepG2 cells infected with pHAGE-Salusin-α lentivirus. (B) The expression of salusin-α and AdipoR2 protein in HepG2 cells infected with pLKO.1-shSalusin-α#1 lentivirus. Data are shown as the mean ± SD. *P<0.05, **P<0.01 and ***P<0.001 by t-test. AdipoR2, adiponectin receptor 2; NC, negative control; shMock, a meaningless RNA as a control for shSalusin-α; shSalusin-α#1, pLKO.1-shSalusin-α#1, representing interference salusin-α; pHAGE-Salusin-α, representing overexpression salusin-α; sh-, short hairpin.

was chosen for subsequent experiments. Furthermore, comparison results of each control group demonstrated that there were no significant difference in the expression level of salusin-α mRNA and protein among the control groups (Fig. 3, P>0.05). Therefore, in the next interference experiment, only shMock was used as the control.

Effects of overexpression and interference with salusin-α on AdipoR2 expression in 293T cells. The mRNA and protein expression of salusin-α and AdipoR2 in the 293T cells were detected by SQ-PCR and WB analysis. It was clearly revealed that, in the cells infected with pHAGE-Salusin-α virus, the expression levels of salusin-α mRNA and protein were significantly increased (P<0.05), as well as the expression levels of AdipoR2 mRNA and protein (Fig. 4A and B). On the other hand, in the cells infected with pLKO.1-shSalusin-α virus, the mRNA and protein levels of salusin-α were significantly reduced (P<0.05), resulting in a significant inhibition of the expression of AdipoR2 (Fig. 4A and C). However, these changes were not observed in the NC, pHAGE or shMock groups (Fig. 4). Collectively, these results demonstrated that salusin-α has a positive regulatory effect on AdipoR2.

Effects of overexpression and interference with salusin-α on AdipoR2 protein expression in HepG2 cells. Subsequently, given the aforementioned results wherein the association between salusin-α and AdipoR2 in 293T cells was studied, and since hepatocytes have an important role in regulating lipid metabolism and salusin-α and AdipoR2 are both involved in lipid metabolism, HepG2 cells were chosen to explore further the association between salusin-α and AdipoR2. The cultured HepG2 cells were infected with pHAGE-Salusin-α, pLKO.1-shSalusin-α#1 and the control virus. After culturing for 48 h, the cells were collected for WB detection. As expected, in this experiment, compared with the non-infected NC group and the infected pHAGE or shMock virus groups, the expression level of AdipoR2 in the HepG2 cells infected with pHAGE-Salusin-α increased significantly (Fig. 5A), whereas the opposite results were obtained in the pLKO.1-shSalusin-α#1 group (Fig. 5B) (all P<0.05). Furthermore, no significant differences were observed among the NC, pHAGE and shMock groups for AdipoR2 expression in HepG2 cells (P>0.05).

Effects of overexpression and interference of salusin-α on the PPARa-ApoA5/SREBP-1c pathway via regulating AdipoR2.

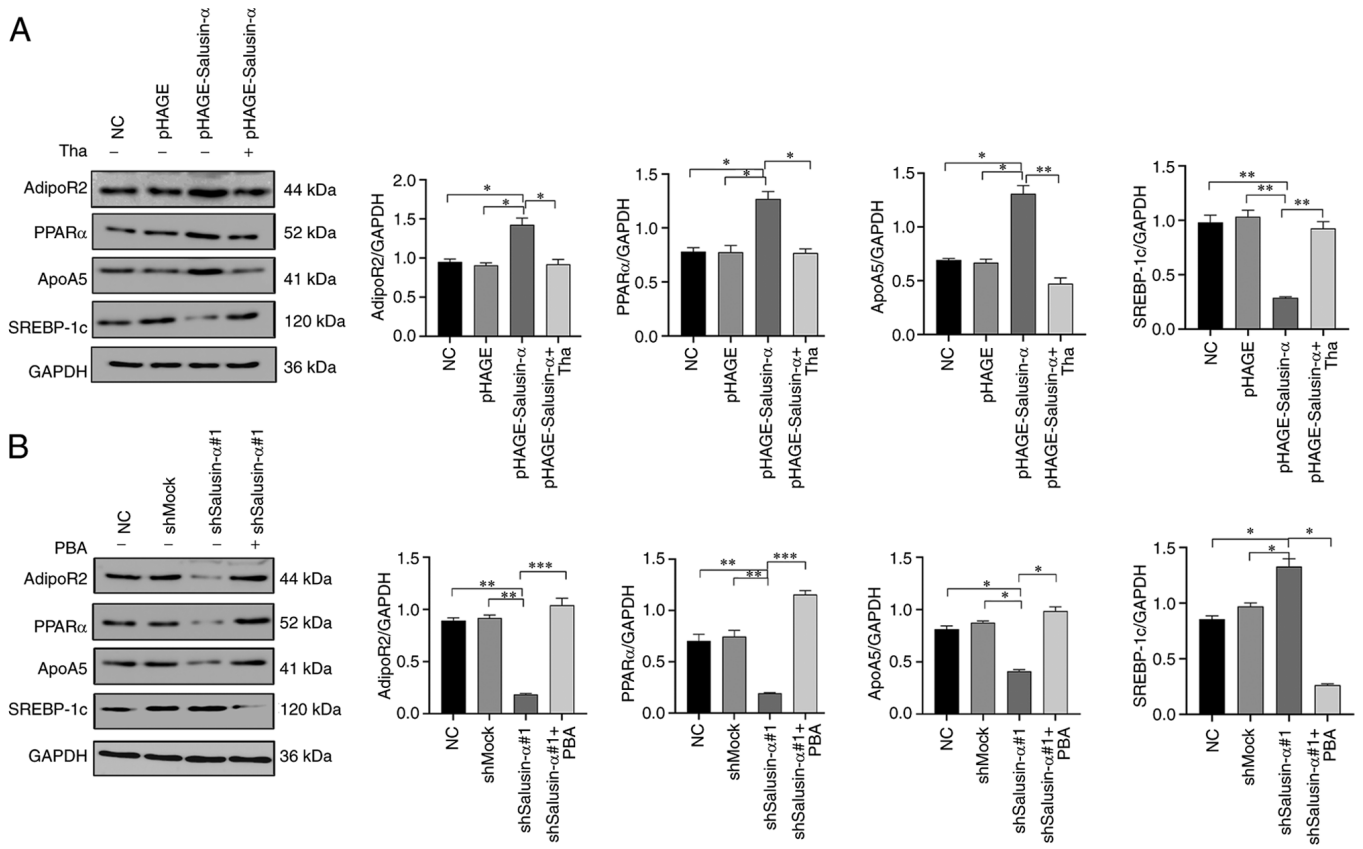

Figure 6. Effects of Salusin-α overexpression or interference on the levels of AdipoR2, APPRα, ApoA5 and SREBP-1c. (A) HepG2 cells were transfected with pHAGE and pHAGE-Salusin-α. Two groups of HepG2 cells infected with pHAGE-Salusin-α, after 24 h of culture, one of the pHAGE-Salusin-α groups was treated with Tha for 24 h, whereas the other groups were continued to cultivate and remained unchanged. WB analysis detected the changes in the levels of AdipoR2, PPARα, ApoA5 and SREBP-1c proteins. (B) HepG2 cells were transfected with shMock and shSalusin-α#1. Two groups of HepG2 cells infected with shSalusin-α#1, then after 24 h, one of the shSalusin-α#1 groups was treated with PBA for 24 h, whereas the other groups were continued to cultivate and remain unchanged. WB analysis detected the changes in the protein levels of AdipoR2, PPARα, ApoA5 and SREBP-1c. The data are presented as the mean ± SD. *P<0.05, **P<0.01 and ***P<0.001 by t-test. NC, negative control; shMock, a meaningless RNA as a control for shSalusin-α; shSalusin-α#1, pLKO.1-shSalusin-α#1, representing interference salusin-α; pHAGE-Salusin-α, representing overexpression salusin-α; Tha, thapsigargin; PBA, 4-phenyl butyric acid; AdipoR2, adiponectin receptor 2; PPARα, peroxisome proliferator-activated receptor-α; ApoA5, apolipoprotein A5; SREBP-1c, sterol regulatory element-binding transcription factor 1; sh-, short hairpin.

In order to further explore whether overexpression of salusin-α can activate the PPARα/ApoA5/SREBP-1c signaling pathway via the regulation of AdipoR2, thereby inhibiting lipid metabolism in HepG2 cells, the effects of overexpression or interference of salusin-α on the expression levels of PPARα, ApoA5 and SREBP-1c by were detected using WB analysis. As demonstrated in Fig. 6A, compared with the NC group, the overexpression of salusin-α led to a significant increase in the expression levels of PPARα and ApoA5in HepG2 cells, although the expression level of SREBP-1c was opposed to PPARα and ApoA5. However, in the pLKO.1-shSalusin-α#1 group, the expression levels of PPARα and ApoA5 were clearly inhibited, whereas the expression of SREBP-1c was moderately increased (Fig. 6B). No significant differences were observed in the expression levels of these proteins in the NC, pHAGE or shMock groups (Fig. 6). Furthermore, it is noteworthy that the changes in the intracellular protein levels after adding thapsigargin and PBA conformed with the anticipated results. After adding thapsigargin to the pHAGE-Salusin-α group, the expression of AdipoR2 was significantly decreased compared with the pHAGE-Salusin-α group without thapsigargin treatment, as well as the protein levels of PPARα and ApoA5, although the SREBP-1c protein level increased, reversing the changes of these protein levels caused by the increase in salusin-α protein level (Fig. 6A). However, co-incubation of PBA with HepG2 cells infected with pLKO.1-shSalusin-α#1 led to a clear increase in the expression levels of AdipoR2, PPARα and ApoA5, although the levels of SREBP-1c protein decreased, which were the opposite of the changes of these protein levels caused by the decrease of salusin-α protein level (Fig. 6B). Taken together, these data clearly confirmed that overexpression of salusin-α could inhibit lipid metabolism in HepG2 cells through upregulating AdipoR2 expression to activate the PPARα-ApoA5/SREBP-1c signaling pathway.

Discussion

Salusin-α and adiponectin are two bioactive peptides that are associated with lipid metabolism. Previous studies have shown that adiponectin activates PPARα by binding with AdipoR2, thereby effecting changes in downstream molecules associated with lipid synthesis (9,17,18). Notably, salusin-α has also been shown to cause an increase in the expression of PPARα signaling molecules in hepatocytes, thereby inhibiting lipid

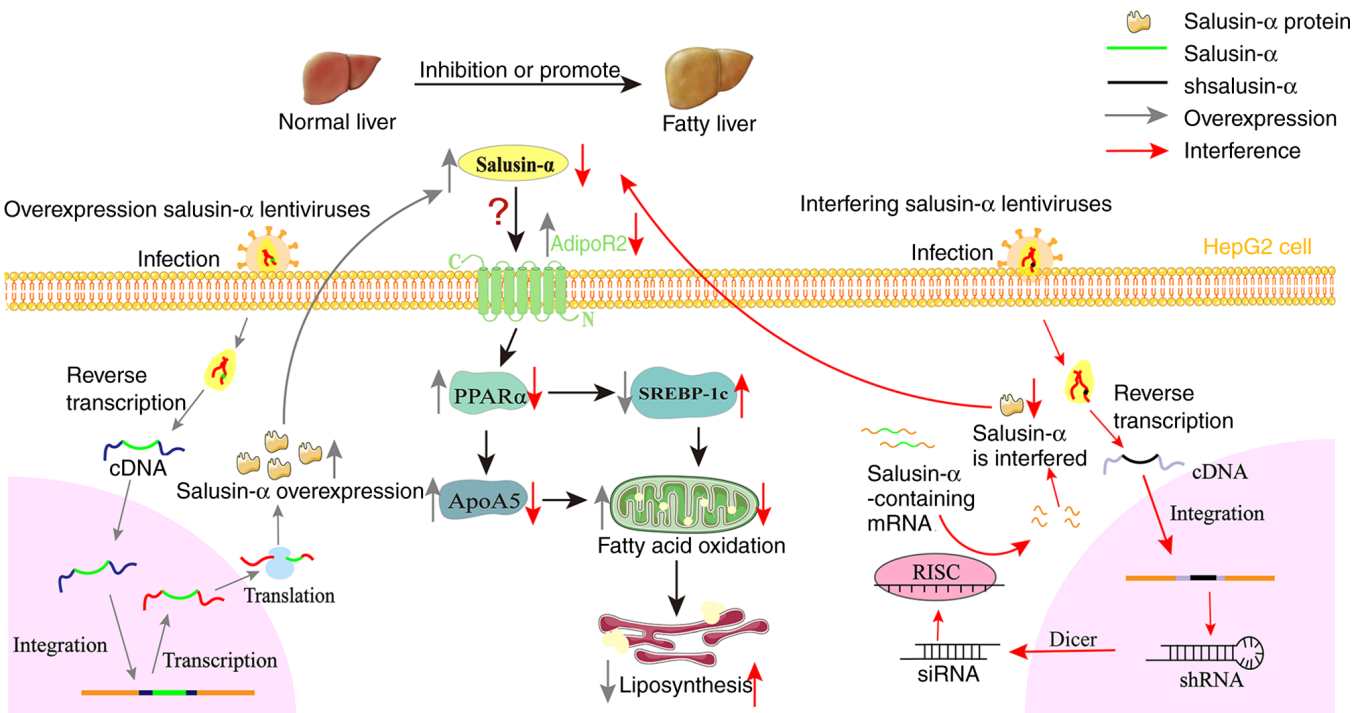

Figure 7. Overexpression of salusin-α upregulates AdipoR2 and activates the PPARα/ApoA5/SREBP-1c pathway. Based on the present study, the following hypothesis is proposed: Salusin-α and the interference sequences were transported into cells by lentivirus, and after a series of modification, the expression level of salusin-α was changed. Salusin-α can influence AdipoR2, and its overexpression leads to upregulation of the AdipoR2 expression level, thereby upregulating the expression of PPARα in hepatocytes, whereas PPARα upregulates the expression of ApoA5 and inhibits the expression of SREBP-1c, ultimately promoting fatty acid oxidation and reducing lipid accumulation in hepatocytes. There are numerous possibilities that could account for how salusin-α interacts with AdipoR2: It may be that salusin-α directly binds with AdipoR2 and activates it, or salusin-α indirectly acts on AdipoR2 through adiponectin, and so on; these aspects need to be confirmed by subsequent research. The gray arrow represents the mechanism process of overexpression lentivirus transporting salusin-α and regulating salusin-α expression. The red arrow represents the mechanism process that interferes with the lentivirus to transport the interfering sequence of salusin-α and thus regulates salusin-α. shsalusin-α, Interference sequence of salusin-α. PPARα, peroxisome proliferator-activated receptor-α; ApoA5, apolipoprotein A5; SREBP-1c, sterol regulatory element-binding transcription factor 1; AdipoR2, adiponectin receptor 2; sh-, short hairpin.

synthesis in hepatocytes (19). However, to date, few studies have reported on whether salusin-α can elicit changes in PPARα mediated through AdipoR2. In the present study, for the first time to the best of our knowledge, the association between salusin-α and AdipoR2 was explored by synthesizing overexpression and interfering salusin-α lentivirus vectors in 293T cells, which revealed that salusin-α overexpression could upregulate AdipoR2, leading to the activation of the PPARα/ApoA5/SREBP-1c signaling pathway to inhibit lipid synthesis in HepG2 cells.

In recent years, salusin-α and adiponectin are two vasoactive peptides that have been found to inhibit atherosclerosis. A previous study showed that dyslipidemia is an important risk factor for atherosclerosis (21). It is well-established that the liver fulfills important roles in the processes of lipid metabolism. Excessive cholesterol and lipid accumulation will lead to a liver overload, resulting in liver lipid metabolism disorder and forming fatty liver, which then induces atherosclerosis (19,22,23). Therefore, how to interfere with that lipid metabolism disorder, thereby inhibiting lipid accumulation in liver cells and to prevent fatty liver and atherosclerosis, is a current 'hot spot' in clinical research. PPARα is a signaling molecule that is associated with lipid metabolism in liver cells, and regulated by adiponectin through AdipoR2 (24). A large number of studies have shown that AdipoR2 is predominantly expressed in the liver, mainly acting on PPARα (9,17,18,25). However, salusin-α inhibits lipid synthesis in hepatocytes through PPARα (19), although it remains unclear whether salusin-α regulation could affect PPARα via AdipoR2. It was surmised that salusin-α could regulate lipid metabolism by AdipoR2; therefore, in these experiments, differently from the previous injection of salusin-α protein into mice (19), the lentivirus system was used to transfer the salusin-α gene into the cell chromosome to achieve long-term expression of the target protein. First, the overexpression and interference salusin-α recombinant plasmids were constructed, after which they were packaged into 293T cells with the creation of overexpression and interference salusin-α lentiviruses for the infection of target cells, with the aim of directly upregulating or inhibiting the expression of salusin-α in cells at the genetic level. In addition, the target gene introduced by lentiviral construction could be stably expressed in cells without disappearing as a consequence of cell division (26,27). Another advantage was that this system also eliminated experimental interference caused by other human factors, rendering it more a more accurate and convenient method for detecting subsequent signal pathway molecules.

In order to verify the aforementioned hypothesis, the synthetic overexpression and interfering salusin-α viruses were first transfected into 293T cells. First, 23 pairs of primers were designed for peptide genes associated with atherosclerosis, and the correlation between the expression of these genes

and the overexpression of salusin-α gene was detected using the RT-qPCR method (data not shown). The results obtained showed that the overexpression of salusin-α caused a significant promotion of the expression of AdipoR2, whereas interfering with salusin-α expression effectively inhibited the expression of AdipoR2, indicating that there was a certain association between salusin-α and AdipoR2. Regarding salusin-α, it was still unknown whether it could directly act on AdipoR2 or indirectly act on AdipoR2 through adiponectin or other molecules, and this problem required additional investigations to confirm the nature of the association. Furthermore, since salusin-α and AdipoR2 are closely associated with lipid metabolism and the liver is an important site of lipid metabolism, HepG2 cells were chosen for subsequent experiments. As expected, after infecting HepG2 cells with salusin-α overexpression and interference lentivirus, the changes of AdipoR2 were consistent with those in 293T cells. Furthermore, according to previous studies (28,29), there are a number of cell signaling pathways that are considered to be involved in lipid synthesis in hepatocytes, among which the PPARα/ApoA5/SREBP-1c signaling pathway is one of the most important. In addition, a range of studies have confirmed that AdipoR2 can promote ApoA5, or inhibit the expression of SREBP-1c, by activating PPARα, inhibiting lipid synthesis and thereby reducing the excessive accumulation of lipid in hepatocytes (30,31). Whether salusin-α can inhibit lipid synthesis in hepatocytes through regulating the PPARα/ApoA5/SREBP-1c signaling pathway via upregulating AdipoR2 has rarely been reported. Based on the research aims of the present study, the overexpression and interference salusin-α viruses were transferred into HepG2 cells, and it was subsequently found that, after infection with overexpression salusin-α lentivirus, the expression levels of AdipoR2, PPARα and ApoA5 in HepG2 cells were increased, whereas that of SREBP-1c was decreased. However, in HepG2 cells infected with interfering salusin-α lentivirus, the opposite results were obtained. Moreover, in order to confirm that the changes in the levels of PPARα, ApoA5 and SREBP-1c were caused by the changes in the level of AdipoR2, the inhibitor (thapsigargin) and the agonist (PBA) of AdipoR2 were also added in subsequent experiments (20,32). Thapsigargin is an endoplasmic reticulum stress inducer which has been shown to induce an increase of ATF3 transcription; furthermore, ATF3 is able to bind to a segment of the AdipoR2 promoter to inhibit the expression of AdipoR2 (20). Therefore, thapsigargin reduces the expression of AdipoR2. After the addition of AdipoR2 inhibitors, it was found that the expression of AdipoR2, PPARα and ApoA5 in HepG2 cells was decreased, whereas that of SREBP-1c was increased. By contrast, PBA was found to reduce endoplasmic reticulum stress and lower the expression level of ATF3, thereby promoting the expression of AdipoR2 (33). The findings of the present study revealed that, after the addition of the AdipoR2 agonist, the expression levels of AdipoR2, PPARα and ApoA5 in HepG2 cells were increased, whereas that of SREBP-1c was decreased. It must be acknowledged that, in the present study, shSalusin-α#1 did not completely abolish the influence of salusin-α; therefore, whether salusin-α possibly exerts a different role through other signaling pathways requires further study.

Based on all the information and data in the present study, it is possible to propose a new hypothesis whereby salusin-α alters the expression of AdipoR2, and thereby regulates lipid metabolism through the PPARα/ApoA5/SREBP-1c signaling pathway (Fig. 7). Overexpression of salusin-α may promote the increase in AdipoR2 expression, and activate PPARα. PPARα is a type of nuclear transcription factor, which is able to promote the metabolism of chyle particles and very low-density lipoprotein, promote the hydrolysis of TG and fatty acid oxidation (34-36). In addition, PPARα has two functions; on the one hand, it can combine with ApoA5 to promote an increase in ApoA5 expression, and on the other hand, it is able to inhibit the expression of SREBP-1c. ApoA5 is a relatively new member of apolipoprotein superfamily, discovered in 2001, which has been shown to be associated with the content of TG, and it is also the only known apolipoprotein that can reduce plasma TG (17,37). Notably, SREBP-1c regulates the expression of several enzymes that catalyze the synthesis of fatty acids, cholesterol, TG and phospholipids (18,38,39). Ultimately, both of these actions result in an increase in fatty acid oxidation, thereby leading to the decomposition of intracellular lipids. In the current series of experiments, it was found that an increase in salusin-α expression upregulated AdipoR2, which in turn activated the PPARα/ApoA5/SREBP-1c signaling pathway, thereby regulating lipid metabolism. However, how salusin-α interacts with AdipoR2 remains unclear, and the present study has only featured *in vitro* experiments; therefore, further studies are required to reveal the mode of action between salusin-α and AdipoR2.

In conclusion, in the present study, it was reported for the first time to the best of our knowledge, that overexpression of salusin-α inhibits lipid anabolism in HepG2 cells through upregulating AdipoR2, resulting in the activation of the PPARαApoA5/SREBP-1c signaling pathway. Therefore, salusin-α is a potential target molecule associated with lipid metabolism that may be recruitable in clinical interventions targeted against atherosclerosis.

Acknowledgements

The authors are grateful to Dr Duan Qiuhong (Department of Basic Medicine of Wuhan Huazhong University of Science and Technology) for providing the lentiviral plasmids and 293T cells.

Funding

The present study was supported by the Top 1% of ESI discipline creation projects of Hubei University of Chinese Medicine (grant nos. 100702020506 and 100702020518) and the Research Plan Projects of the Hubei Provincial Department of Education (grant no. B2018099).

Availability of data and materials

The datasets used and/or analyzed during the current study are available from the corresponding author on reasonable request.

Authors' contributions

YW and HZ designed the study and confirm the authenticity of all the raw data. CY and GG performed the sequencing

experiments and provided critical advice during the preparation of the manuscript. HZ, AX, SW, QZ and XD prepared materials, collected data and performed analysis. All authors commented on previous versions of the manuscript, and read and approved the final manuscript.

Ethics approval and consent to participate

Not applicable.

Patient consent for publication

Not applicable.

Competing interests

The authors declare that they have no competing interests.

References

1. Shichiri M, Ishimaru S, Ota T, Nishikawa T, Isogai T and Hirata Y: Salusins: Newly identified bioactive peptides with hemodynamic and mitogenic activities. Nat Med 9: 1166-1172, 2003.
2. Suzuki N, Shichiri M, Akashi T, Sato K, Sakurada M, Hirono Y, Yoshimoto T, Koyama T and Hirata Y: Systemic distribution of salusin expression in the rat. Hypertens Res 30: 1255-1262, 2007.
3. Raposeiras-Roubin S, Rosselló X, Oliva B, Fernández-Friera L, Mendiguren JM, Andrés V, Bueno H, Sanz J, Martínez de Vega V, Abu-Assi E, *et al*: Triglycerides and residual atherosclerotic risk. J Am Coll Cardiol 77: 3031-3041, 2021.
4. Qian K, Feng L, Sun Y, Xiong B, Ding Y, Han P, Chen H, Chen X, Du L and Wang Y: Overexpression of Salusin-α inhibits vascular intimal hyperplasia in an atherosclerotic rabbit model. Biomed Res Int 2018: 8973986, 2018.
5. Niepolski L and Grzegorzewska AE: Salusins and adropin: New peptides potentially involved in lipid metabolism and atherosclerosis. Adv Med Sci 61: 282-287, 2016.
6. Grzegorzewska AE, Niepolski L, Sikora J, Janków M, Jagodziński PP and Sowińska A: Effect of lifestyle changes and atorvastatin administration on dyslipidemia in hemodialysis patients: A prospective study. Pol Arch Med Wewn 124: 443-451, 2014.
7. Fang H and Judd RL: Adiponectin regulation and function. Compr Physiol 8: 1031-1063, 2018.
8. Parida S, Siddharth S and Sharma D: Adiponectin, obesity, and cancer: Clash of the Bigwigs in health and disease. Int J Mol Sci 20: 2519, 2019.
9. Zha D, Wu X and Gao P: Adiponectin and its receptors in diabetic kidney disease: Molecular mechanisms and clinical potential. Endocrinology 158: 2022-2034, 2017.
10. Lee IK, Kim G, Kim DH and Kim BB: PEG-BHD1028 peptide regulates insulin resistance and fatty acid β-oxidation, and mitochondrial biogenesis by binding to two heterogeneous binding sites of adiponectin receptors, AdipoR1 and AdipoR2. Int J Mol Sci 22: 884, 2021.
11. Furukawa K, Hori M, Ouchi N, Kihara S, Funahashi T, Matsuzawa Y, Miyazaki A, Nakayama H and Horiuchi S: Adiponectin down-regulates acyl-coenzyme A: Cholesterol acyltransferase-1 in cultured human monocyte-derived macrophages. Biochem Biophys Res Commun 317: 831-836, 2004.
12. Yanai H and Yoshida H: Beneficial effects of adiponectin on glucose and lipid metabolism and atherosclerotic progression: Mechanisms and perspectives. Int J Mol Sci 20: 1190, 2019.
13. Ipsen DH, Lykkesfeldt J and Tveden-Nyborg P: Molecular mechanisms of hepatic lipid accumulation in non-alcoholic fatty liver disease. Cell Mol Life Sci 75: 3313-3327, 2018.
14. Younossi ZM, Corey KE and Lim JK: AGA clinical practice update on lifestyle modification using diet and exercise to achieve weight loss in the management of nonalcoholic fatty liver disease: Expert review. Gastroenterology 160: 912-918, 2021.
15. Perakakis N, Stefanakis K and Mantzoros CS: The role of omics in the pathophysiology, diagnosis and treatment of non-alcoholic fatty liver disease. Metabolism 111: 154320, 2020.
16. Scherer A and Dufour JF: Treatment of non-alcoholic fatty liver disease. Dig Dis 34: 2731, 2016.
17. Alborn WE, Johnson MG, Prince MJ and Konrad RJ: Definitive N-terminal protein sequence and further characterization of the novel apolipoprotein A5 in human serum. Clin Chem 52: 514-517, 2006.
18. Peng CH, Yang MY, Yang YS, Yu CC and Wang CJ: Antrodia cinnamomea prevents obesity, dyslipidemia, and the derived fatty liver via regulating AMPK and SREBP signaling. Am J Chin Med 45: 6783, 2017.
19. Tang K, Wang F, Zeng Y, Chen X and Xu X: Salusin-α attenuates hepatic steatosis and atherosclerosis in high fat diet-fed low density lipoprotein receptor deficient mice. Eur J Pharmacol 830: 7686, 2018.
20. Koh IU, Lim JH, Joe MK, Kim WH, Jung MH, Yoon JB and Song J: AdipoR2 is transcriptionally regulated by ER stress-inducible ATF3 in HepG2 human hepatocyte cells. FEBS J 277: 2304-2317, 2010.
21. Poznyak A, Grechko AV, Poggio P, Myasoedova VA, Alfieri V and Orekhov AN: The diabetes mellitus-atherosclerosis connection: The role of lipid and glucose metabolism and chronic inflammation. Int J Mol Sci 21: 1835, 2020.
22. Qian H, Chao X, Williams J, Fulte S, Li T, Yang L and Ding WX: Autophagy in liver diseases: A review. Mol Aspects Med 82: 100973, 2021.
23. Dong Y, Yu C, Ma N, Xu X, Wu Q, Lu H, Gong L, Chen J and Ren J: MicroRNA-379-5p regulates free cholesterol accumulation and relieves diet induced-liver damage in db/db mice via STAT1/HMGCS1 axis. Mol Biomed 3: 25, 2022.
24. Yang Q, Zhang Y, Li L, Li J, Li Y, Han L and Wang M: D-chiro-Inositol facilitates adiponectin biosynthesis and activates the AMPKα/PPARs pathway to inhibit high-fat diet-induced obesity and liver lipid deposition. Food Funct 13: 7192-7203, 2022.
25. Tomita K, Oike Y, Teratani T, Taguchi T, Noguchi M, Suzuki T, Mizutani A, Yokoyama H, Irie R, Sumimoto H, *et al*: Hepatic AdipoR2 signaling plays a protective role against progression of nonalcoholic steatohepatitis in mice. Hepatology 48: 458-473, 2008.
26. Moreira AS, Cavaco DG, Faria TQ, Alves PM, Carrondo MJT and Peixoto C: Advances in Lentivirus purification. Biotechnol J 16: e2000019, 2021.
27. Yew CT, Gurumoorthy N, Nordin F, Tye GJ, Wan Kamarul Zaman WS, Tan JJ and Ng MH: Integrase deficient lentiviral vector: Prospects for safe clinical applications. PeerJ 10: e13704, 2022.
28. Prieur X, Coste H and Rodriguez JC: The human apolipoprotein AV gene is regulated by peroxisome proliferator-activated receptor-alpha and contains a novel farnesoid X-activated receptor response element. J Biol Chem 278: 25468-25480, 2003.
29. Joshi A, Upadhyay KK, Vohra A, Shirsath K and Devkar R: Melatonin induces Nrf2-HO-1 reprogramming and corrections in hepatic core clock oscillations in non-alcoholic fatty liver disease. FASEB J 35: e21803, 2021.
30. Kim M, Kim M, Yoo HJ, Bang YJ, Lee SH and Lee JH: Apolipoprotein A5 gene variants are associated with decreased adiponectin levels and increased arterial stiffness in subjects with low high-density lipoprotein-cholesterol levels. Clin Genet 94: 438-444, 2018.
31. Wen F, An C, Wu X, Yang Y, Xu J, Liu Y, Wang C, Nie L, Fang H and Yang Z: MiR-34a regulates mitochondrial content and fat ectopic deposition induced by resistin through the AMPK/PPARα pathway in HepG2 cells. Int J Biochem Cell Biol 94: 133-145, 2018.
32. Yu S, Gao L, Zhang C, Wang Y, Lan H, Chu Q, Li S and Zheng X: Glycine ameliorates endoplasmic reticulum stress induced by thapsigargin in porcine oocytes. Front Cell Dev Biol 9: 733860, 2021.
33. Ozcan U, Yilmaz E, Ozcan L, Furuhashi M, Vaillancourt E, Smith RO, Görgün CZ and Hotamisligil GS: Chemical chaperones reduce ER stress and restore glucose homeostasis in a mouse model of type 2 diabetes. Science 313: 1137-1140, 2006.
34. Sinha RA, Rajak S, Singh BK and Yen PM: Hepatic lipid catabolism via PPARα-lysosomal crosstalk. Int J Mol Sci 21: 2391, 2020.
35. Lee YH, Jang HJ, Kim S, Choi SS, Khim KW, Eom HJ, Hyun J, Shin KJ, Chae YC, Kim H, *et al*: Hepatic MIR20B promotes nonalcoholic fatty liver disease by suppressing PPARA. Elife 10: e70472, 2021.

36. Brocker CN, Patel DP, Velenosi TJ, Kim D, Yan T, Yue J, Li G, Krausz KW and Gonzalez FJ: Extrahepatic PPARα modulates fatty acid oxidation and attenuates fasting-induced hepatosteatosis in mice. J Lipid Res 59: 2140-2152, 2018.
37. Luo F, Guo Y, Ruan GY, Peng R and Li XP: Estrogen lowers triglyceride via regulating hepatic APOA5 expression. Lipids Health Dis 16: 72, 2017.
38. Ferré P, Phan F and Foufelle F: SREBP-1c and lipogenesis in the liver: An update1. Biochem J 478: 3723-3739, 2021.
39. Li L, Zhang X, Ren H, Huang X, Shen T, Tang W, Dou L and Li J: miR-23a/b-3p promotes hepatic lipid accumulation by regulating SREBP-1c and Fas. J Mol Endocrinol 68: 3549, 2021.